(NASA-TM-86161) CURRENT CARRIERS FOR THE FIELD-ALIGNED CURRENT SYSTEM (NASA) 21 p HC A02/MF A01 CSCL 03B

N85-17925

Unclas

G3/93 13824

NASA

Technical Memorandum 86161

CURRENT CARRIERS FOR THE FIELD-ALIGNED CURRENT SYSTEM

R. A. Hoffman, M. Sugiura and N. C. Maynard

SEPTEMBER 1984

National Aeronautics and
Space Administration

Goddard Space Flight Center
Greenbelt, Maryland 20771

NASA Technical Memorandum 86161

Current Carriers for the Field-Aligned Current System*

R. A. Hoffman, M. Sugiura and N. C. Maynard

Laboratory for Extraterrestrial Physics

September 1984

*Invited Paper: Symposium on the Physics of the Magnetosphere-Ionosphere Connection
Twenty-fifth Plenary Meeting, Committee on Space Research
Graz, Austria, July 1984

National Aeronautics and Space Administration
Goddard Space Flight Center
Greenbelt, MD 20771

CURRENT CARRIERS FOR THE FIELD-ALIGNED CURRENT SYSTEM

R. A. Hoffman, M. Sugiura and N.C. Maynard

Laboratory for Extraterrestrial Physics
Goddard Space Flight Center
Greenbelt, MD 20771 USA

ABSTRACT

Recently the Dynamics Explorer satellites have returned a large body of data containing high resolution magnetometer measurements and distributions of charged particles of all but thermal electrons. From these data a systematic study has begun of the relations of the field-aligned currents to particle precipitation structures and the identification of the charge carriers. The data have been separated into three levels of magnetic activity and three local time sectors. Results of this study include the following:

1. During very quiet periods, field-aligned currents exist primarily as fine structure.

2. During onset of substorms, Region 1 and Region 2 become clearly evident but contain significant structure.

3. As magnetic activity subsides, current regions become less distinct, and structure becomes more dominant.

4. The distribution of the upward currents derived from magnetometer data and calculated from suprathermal electron data agree remarkably well in shape but not necessarily in magnitude.

5. At all local times, >5 eV electrons seldom carry most of the upward current.

6. Except for the accelerated Inverted-V electrons, the dominant upward current carriers which are measured are below 500 eV and are distributed in energy.

7. Dusk upward currents (Region 1) are associated with the Boundary Plasma Sheet (BPS).

8. Suprathermal electron bursts are important current carrying structures.

INTRODUCTION

Charged particle and magnetic field observations acquired during the past decade from a variety of satellite and sounding rocket instruments have not only confirmed the presence of field-aligned or Birkeland currents, but have shown them to be an important and permanent element in the system coupling the magnetosphere and ionosphere. The most common detection of the currents has been through the interpretation of the variations in the measured vector magnetic field as a satellite passes through a current region. The most direct method of measuring the currents in a space plasma is to count charge carriers, but this requires the measurement with high time resolution of the complete phase space distribution of both electrons and positive charge carriers.

Because of the large quantity of measurements required and the lack of a readily available technique to measure the currents from thermal electrons, this approach has been rarely used. As a result, the identification of current carriers at the various local times and under different magnetic conditions has to date been sporadic; conclusions have been often expressed in terms of general correlations between current regions and particle precipitation regions /1,2/, or based only on a few cases, though some detailed knowledge of the energy regimes for the current carriers is beginning to emerge /3,4/. On the other hand, a large body of information has accumulated based on data from magnetometers, and from this our knowledge of the characteristics of the total currents has evolved to considerable detail /5,6/.

Recently the Dynamics Explorer satellites /7/ have returned considerable data containing high resolution magnetometer measurements and distributions of charged particles of all but thermal electrons. From these data we have begun a systematic study of the Birkeland current charge carriers as a function of magnetic activity and local time. In this report of initial results we will provide some new insights into the properties of field-aligned currents.

DATA SELECTION

Data used in this study were acquired from the Dynamics Explorer-2 (DE-2) spacecraft, which was placed into a polar orbit (90° inclination) with an initial apogee and perigee of slightly over 1000 and 300 km respectively. All data used were from the northern hemisphere from September of 1981 through January of 1982. Because of the offset of the magnetic poles from the geographic poles, all magnetic local times (MLT) were sampled, though coverage just past post-midnight was sparse.

Data were selected according to three levels of magnetic activity, magnetically very quiet, onset phase of a substorm, and recovery phase of a substorm (Figure 1). The magnetic conditions were identified using ground based auroral zone magnetic records, since the AE index is not yet available.

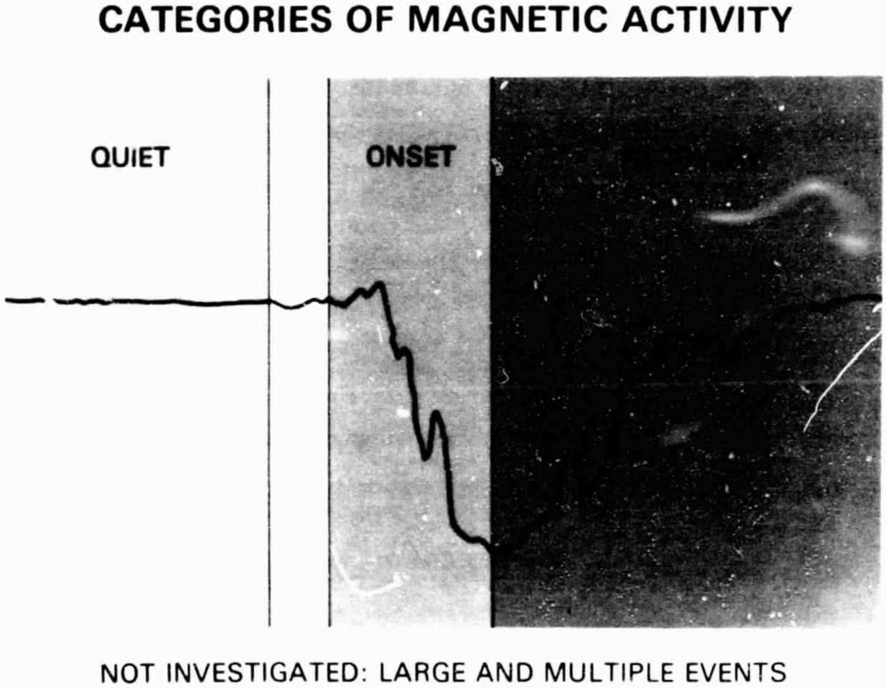

Fig. 1. Schematic illustrating the three levels of magnetic activity for which satellite data were selected for analysis.

Magnetically quiet periods required no fluctuations in the horizontal component in the magnetograms larger than 15 nT for at least two hours before the satellite data were acquired. The onset period was defined from about 15 minutes before the commencement of the negative bay to the maximum of the bay. The recovery period then began, lasting until the return of the horizontal component to pre-storm levels. Data during fairly isolated substorms were sought, whereas data during large and/or complex events were ignored as well as during periods of nondescript magnetic activity.

The selected satellite passes were then further divided into three periods of magnetic local time, the dusk sector, from the cusp to around the Harang discontinuity, the dawn sector, from the Harang to the cusp, and the cusp region, arbitrarily defined as ±2 hours on either side of magnetic noon.

Satellite data used in this study came primarily from the high resolution vector magnetometer (MAG-B) /8/ and low altitude plasma instrument (LAPI) /9/ on DE-2. The magnetometer consisted of triaxial fluxgate sensors mounted on a six-meter mast and provided an instrument resolution of ±1.5 nT over a ±62,000 nT range. The primary sensor used for this study was oriented parallel to the Z-axis of the spacecraft, which was actively controlled to be within a few degrees of orbit normal, and therefore, in an east-west direction geographically. The MAGSAT (1982) magnetic field model was used for subtraction of the ambient field. The LAPI instrument measured electron and total ion fluxes from 5 eV to about 30 keV. It consisted of an array of 15 parabolic electrostatic analyzers spanning 180 in angle and mounted on a one degree-of-freedom scan platform. The platform was controlled by the magnetometer to provide maximum phase-space coverage.

In this presentation, data from specific satellite passes will be shown to illustrate general features found typically under the selected magnetic conditions in the local time sector. Then for each magnetic activity condition, conclusions will be presented based on an analyses of data from many events.

MAGNETICALLY QUIET

The first data illustration is taken from a dusk pass at 1944 MLT during magnetically quiet conditions (Figure 2). The pass began in the polar cap and continued through the auroral oval. The electron spectrogram shows weak structured precipitation which extended over the entire usual polar cap, with Inverted-V structures at low energies at auroral latitudes. A weak, narrow Central Plasma Sheet (CPS) /10/ was encountered from 0042.9 to 0043.7 UT, but during very quiet periods this may not exist at all. The integral over the electron distribution provides the current from the measured electrons. The largest structures in the current occurred at the Inverted-Vs and the CPS.

Currents from the magnetometer are derived from the gradient in the magnetically east-west component of the magnetic difference field assuming the infinite current sheet approximation. The 16 samples/sec magnetometer data were averaged over one second to match the time resolution of the charged particle data. While the magnitudes of the two derived positive (upward) currents differ considerably, many of the larger structures can be found in both data sets. Separate summations of the downward and upward currents derived from the magnetometer data show no major current regions. The total downward current exceeded the upward current, though this may be due to an uncertainty in attitude of the spacecraft, seen as a slow drift in $\Delta B(\Phi)$.

The figure also illustrates the electron regimes which are carrying the portion of the upward current measured by the electron spectrometer. Note from the gradient of the curves that a large portion of the current comes from the Inverted-Vs, whereas the current in the CPS comes from photoelectron energies (12-48 eV), not the CPS particles.

The dawn side of the auroral oval has properties similar to the dusk side, with the current in each direction consisting of fine structure (Figure 3). For this pass the spatial structure of the upward currents derived from both instruments shows excellent agreement in most cases. An integration separately of the upward and downward currents across the primary current region indicates negligible net current, which is apparent from the lack of displacement of the baseline of $\Delta B(\Phi)$ between 0031 and 0036 UT.

The upward current carried by suprathermal electrons resided in the electron energy range 50 eV to 500 eV. Frequently in the morning through cusp local time sector, the electron distributions within photoelectron energies indicate a negative or downward current. The validity of such currents has not been verified, and they are not confirmed by magnetometer data. Note that a small current is carried by mantle (dayside diffuse) auroral electrons /11/ at the lower latitude portion of the auroral oval (energies >480 eV). For this pass the suprathermal electrons carried about 60% of the total upward current in the dawn oval.

During magnetically quiet times most cusp passes displayed characteristics very similar to dawn passes, with very weak mantle auroral electrons on the equatorial side of the oval and weak bursts, either low energy Inverted-Vs or suprathermal bursts /12/ extending from within the mantle region to over the polar cap.

From an analysis of about 75 quiet time passes, the following conclusions have been derived:

1. Field-aligned currents exist primarily as fine structure at all local times. (Region 1 and Region 2 current regions are usually not identifiable.)

2. Structure extends over normal polar cap latitudes.

3. The >5 eV electrons carry the order of 50% of the upward current.

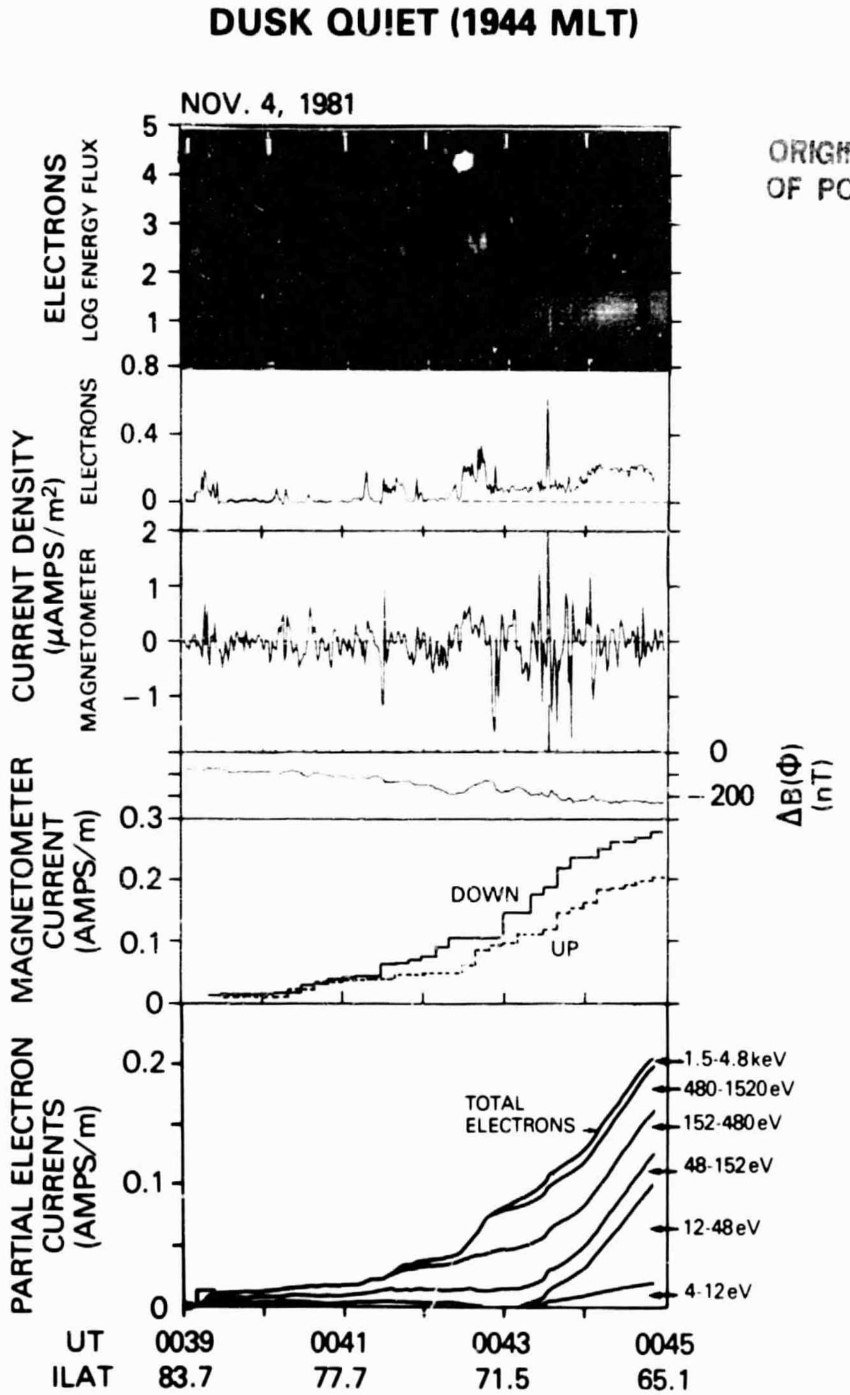

ORIGINAL PAGE IS
OF POOR QUALITY

Fig. 2. Data from Dynamics Explorer-2 during a magnetically quiet period at dusk local time (1944 MLT). The top panel contains a grey scale electron spectrogram from 5 eV to 30 keV measured by the low altitude plasma instrument. Increasing energy fluxes correspond to increasing brightness of the grey scale. The second panel contains the current density (positive is upward current) calculated from the electron distribution. The component of the magnetic field in the magnetic east-west direction with the internal field removed is plotted in the fourth panel. Assuming the infinite current sheet model, the current density derived from the data in panel four is plotted in panel three. Panel five contains separate summations of the upward and downward current densities derived from the magnetometer data, plotted every 10 seconds. Multiplying by the spacecraft velocity gives the integral of the current from one side of the auroral oval to any point within the oval. Similarly, the bottom panel contains separate summations of the electric current density from the electron measurements in a number of energy bands.

ORIGINAL PAGE IS
OF POOR QUALITY

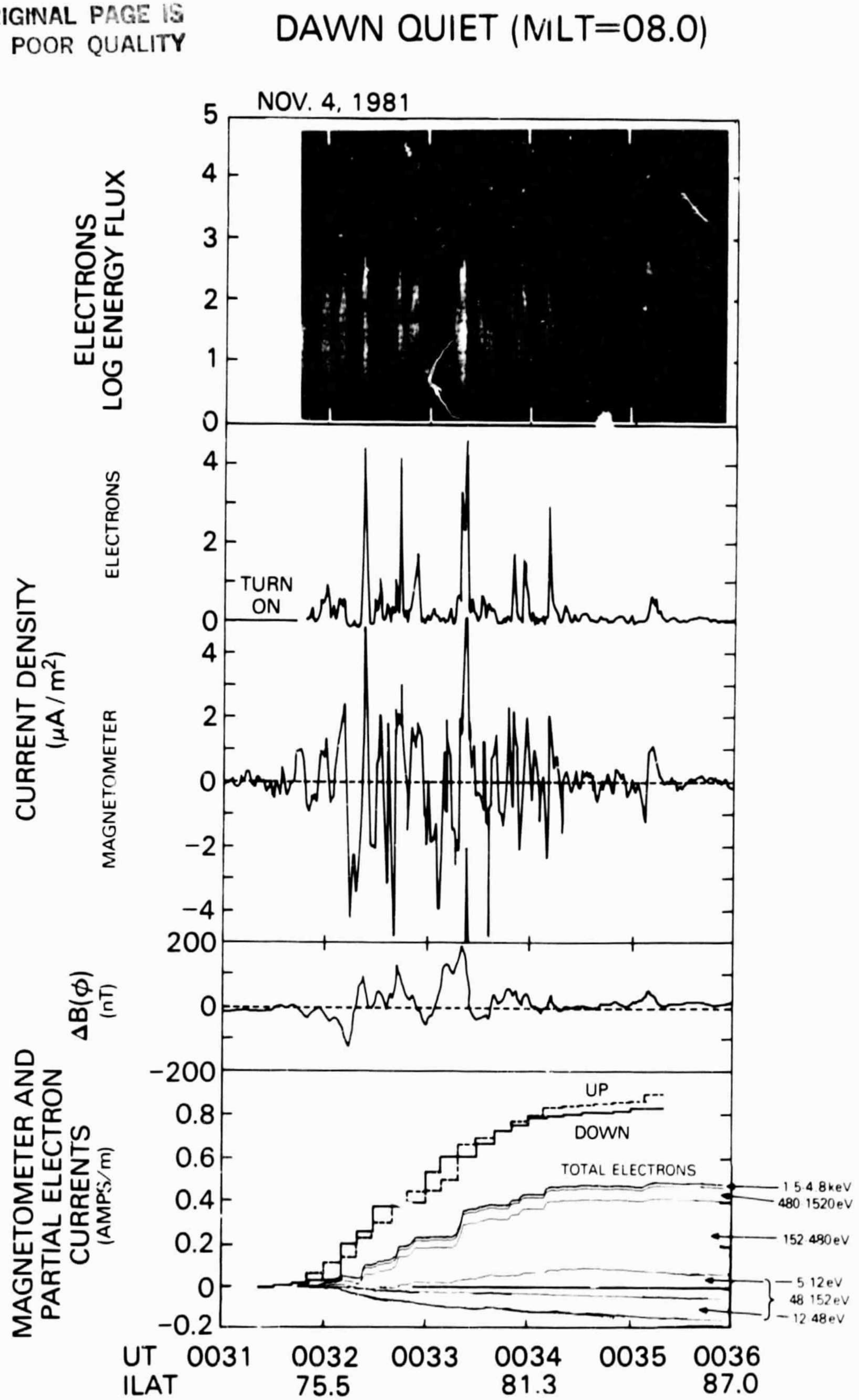

Fig. 3. Format similar to Figure 2 for a pass through the dawn auroral oval during a magnetically quiet period.

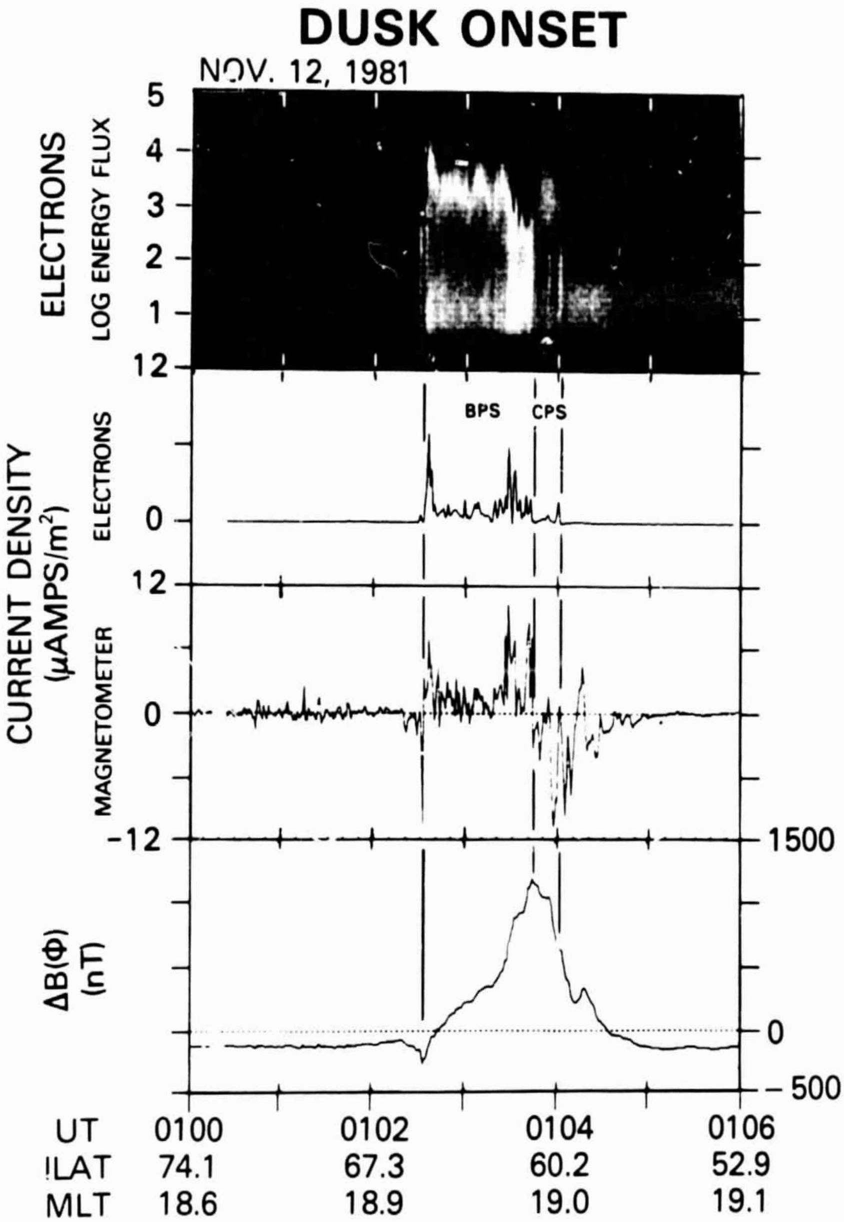

Fig. 4. Format similar to Figure 2 for a pass through the auroral oval during the onset of a substorm, but not including the current sums.

4. The suprathermal electron current carrying range extends from above photoelectron energies to ~500 eV.

5. The source of upward suprathermal electron currents at dusk is the Boundary Plasma Sheet (BPS).

ONSET

During the development of a very sharp bay, the Region 1 and Region 2 currents are clearly evident in the magnetically east-west component of the variation magnetic field (Figure 4). The Region 1 or upward current is exactly coincident with the Boundary Plasma Sheet (BPS). This pattern and relationship are very typical of the dusk hours during substorm onset. In this example, the BPS consisted of two parts, a broad Inverted-V with peak energy at a few keV, and a lower energy, but higher intensity, Inverted-V below 1 keV. Note, however, the considerable structure and even current reversals in each region. The ratio of upward to downward currents in Region 2 was about 15, and the inverse ratio in Region 1 about 9. Also note that the low latitude boundaries of Region 2 and the CPS were not coincident.

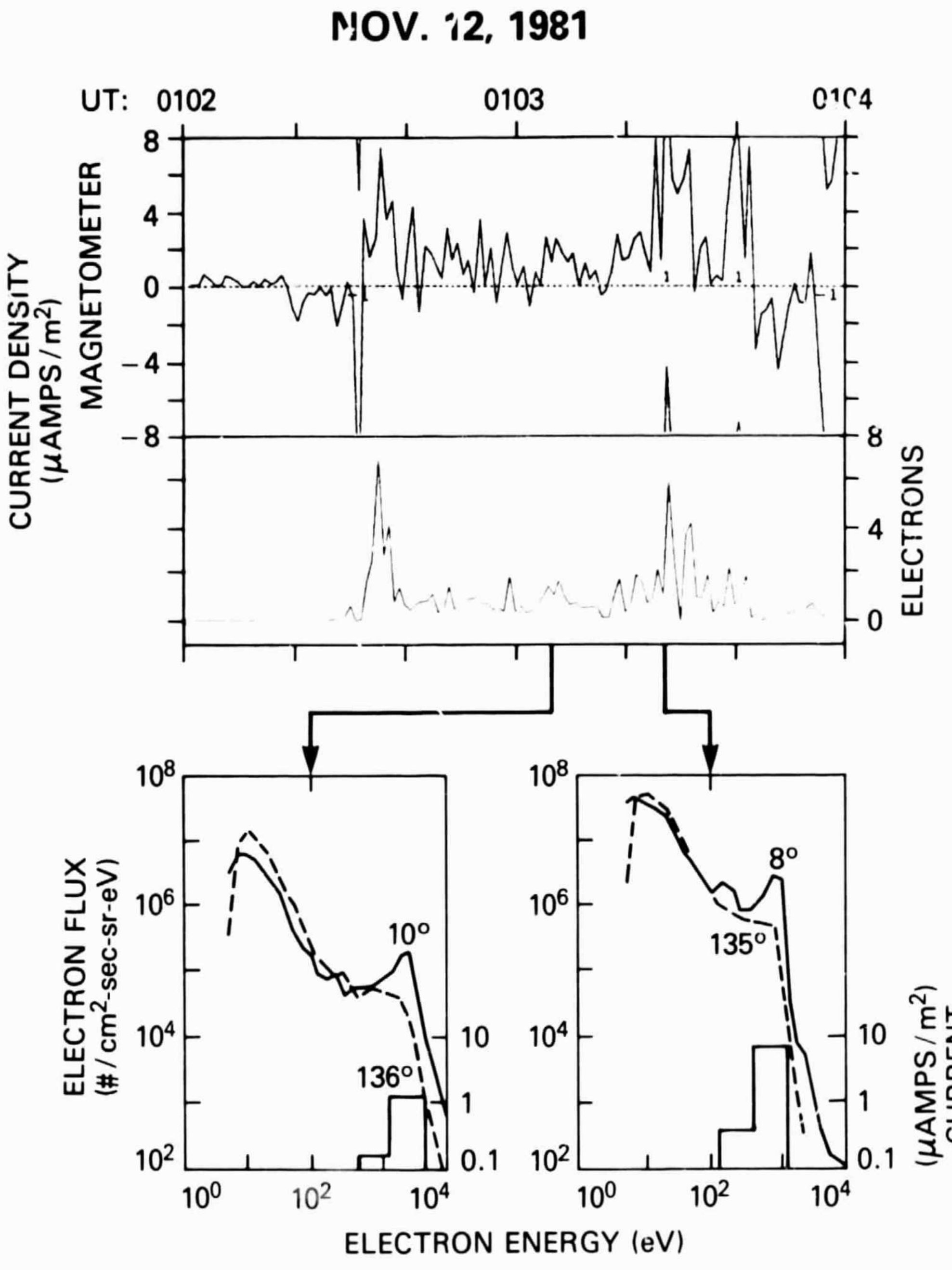

Fig. 5. Current densities from the magnetometer and low altitude plasma data during two minutes of the pass shown in Figure 4. Below are selected energy spectra with the pitch angles labeled and the partial current densities in the energy bands shown in Figure 2.

Concentrating just on the upward current region (Figure 5) we find somewhat better agreement in magnitude between the two methods of deriving the upward current densities than during magnetically quiet periods, except near the very end of the lower energy Inverted-V (around 0103:40 UT). Typical energy spectra are shown in each of the Inverted-Vs. The pitch angle distributions of the precipitating electrons were quite isotropic, characterized by the spectrum at 10° pitch angle, with fairly large upgoing electron fluxes (136° pitch angle). The partial current densities show clearly that the current was carried by the accelerated electrons.

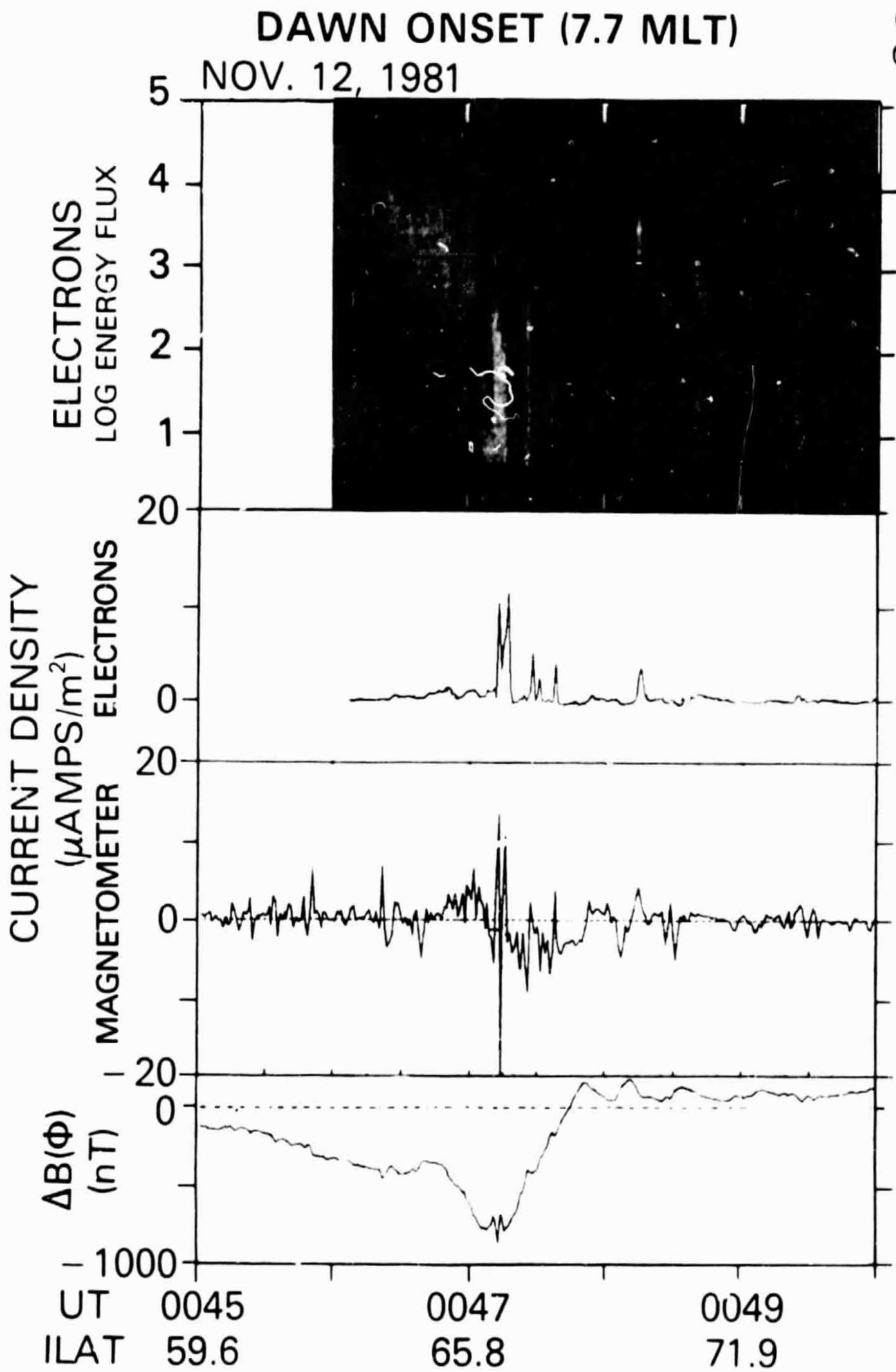

Fig. 6. Format similar to Figure 4 for a pass through the dawn auroral oval during the onset phase of a substorm.

On the dawn side, a very patchy mantle (diffuse) auroral electron precipitation region seen at the beginning of the spectrogram (Figure 6) provided weak upward (Region 2) currents and ended very abruptly, followed by a very sharp, low energy double burst with a large current reversal in the center (0047:15 UT) according to the magnetometer data. A good majority of the upward current integrated across the auroral oval was contained in this burst. Note that there was no sharp polar cap boundary, but weak bursts and currents extending to over 80° invariant latitude. There was a very small net upward current across the dawn-side oval when compared to the separate upward and downward current sums, in keeping with Sugiura et al's /13/ finding that most of the field-aligned current closes in the ionosphere via Pederson currents.

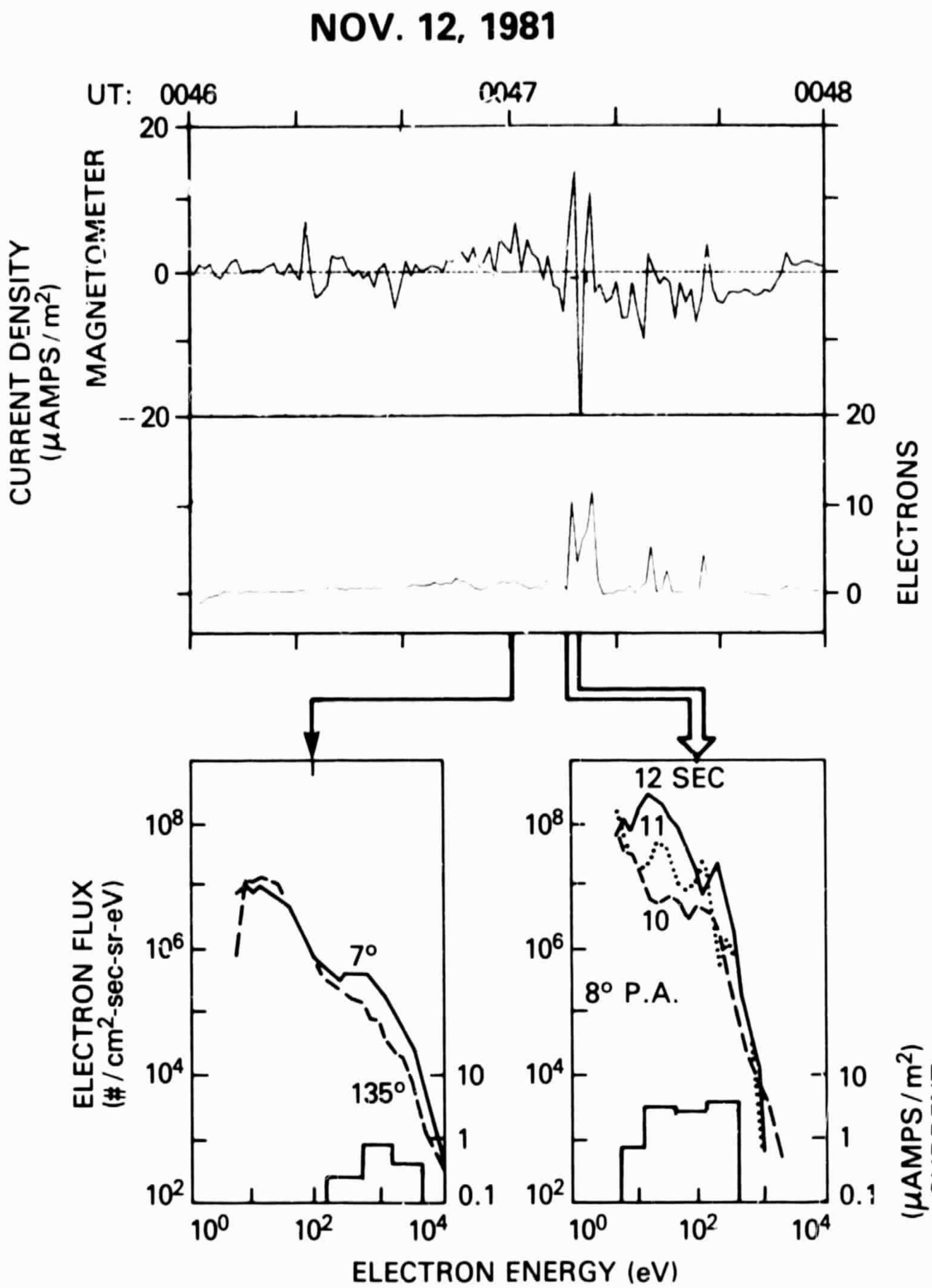

Fig. 7. Format similar to Figure 5 for two minutes of the pass shown in Figure 6. The partial current density plotted in the lower right panel was for second 12.

Again looking in detail at the key portion of the pass (Figure 7), the energy spectra in the more intense portion of the mantle auroral region (lower left spectra) shows the current carriers spread across the electron energy range from about 100 eV well into the kilovolt region. This is typical, provided the electrons have drifted already from the nightside injection region to the local time of the morning observation. Because the double bursts were very narrow it is difficult to determine their energy spectra. Three spectra are shown for each second leading to the first peak, but the spectra are aliased because of the rapid time variations. It appears that the first burst may have been an Inverted-V, but the second was probably a suprathermal burst.

DUSK ONSET

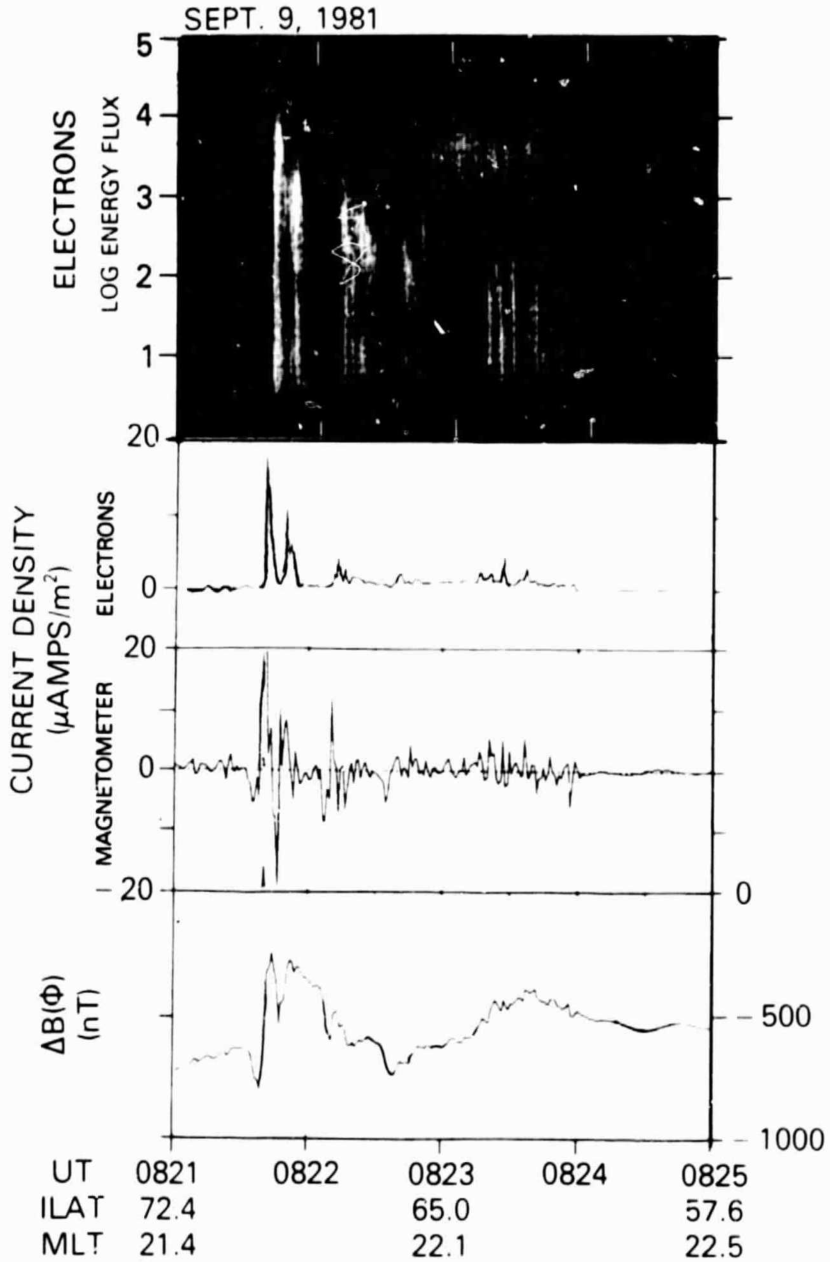

Fig. 8. Data from a dusk pass closer to midnight than the example shown in Figure 4 in a format similar to Figure 4.

A second dusk pass closer to midnight than the first onset example showed a more complex pattern of currents, or multiple current sheets (Figure 8) which is typical under these conditions /5/. The high latitude boundary of precipitation was dominated by two sharp bursts of electrons, with a current reversal seen in the magnetometer data. The boundary between the CPS and BPS is not clearly defined, because there was a region of mixture of Inverted-Vs, diffuse CPS plasma and even suprathermal bursts /12/ which extended to the low latitude boundary of the CPS.

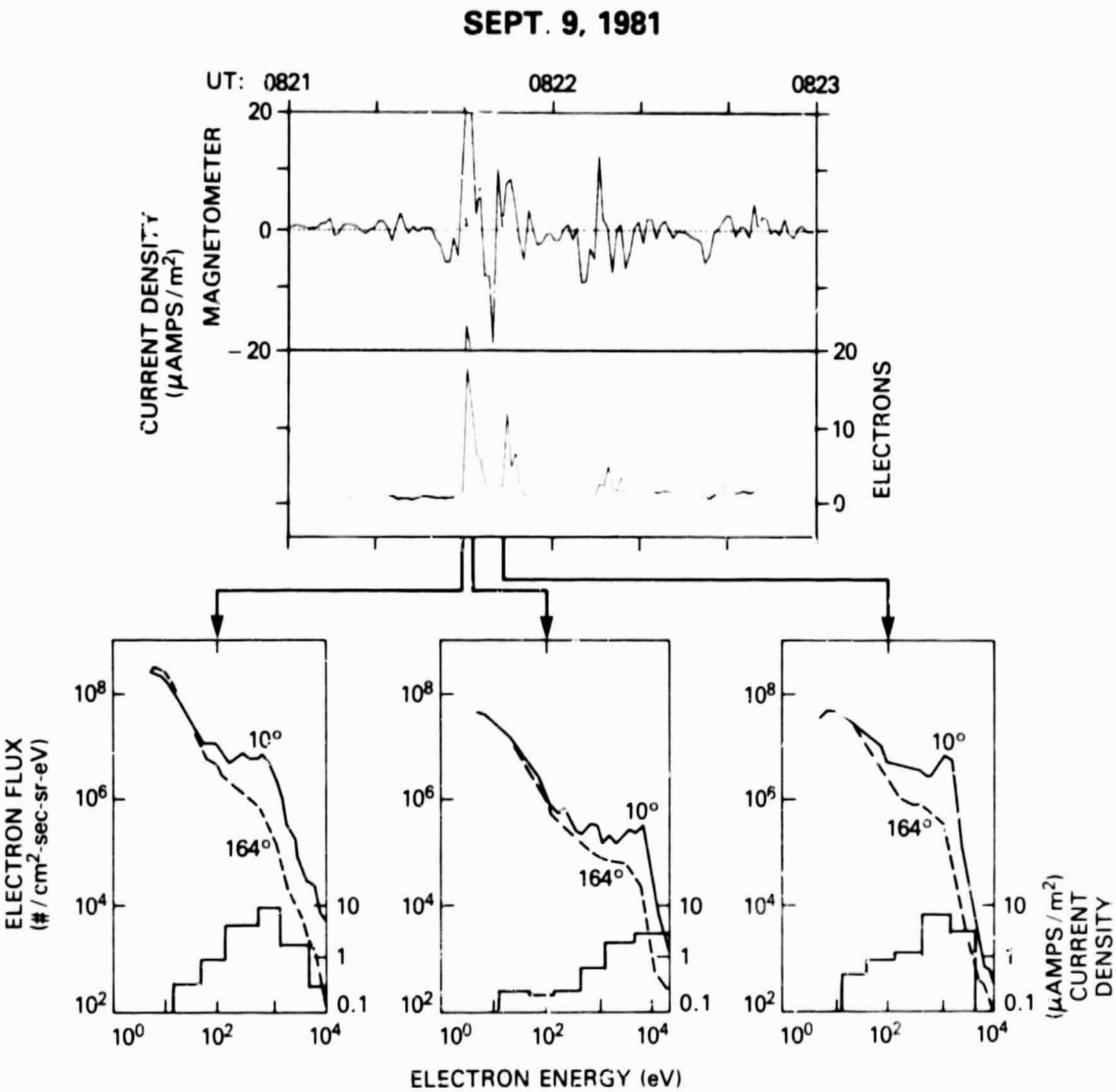

Fig. 9. Format similar to Figure 5 for two minutes of the pass shown in Figure 8.

Looking again in detail at the intense current region (Figure 9), the rapid encounter of the high latitude burst makes identification difficult. This onset of auroral particles does not show signs of the characteristic sharp peak in the spectrum of an Inverted-V (left spectra), although the spectrum two seconds later (center spectra) and the second burst (right spectra) are clearly Inverted-Vs. Noting that the log of the partial currents is plotted, most of the current appeared in the accelerated electrons, but at the onset it was more distributed.

The cusp precipitation pattern during the development of a substorm appears considerably different from the pattern during dawn passes (Figure 10). While very structured precipitation with energies of a few hundred eV extended to high latitudes, most of the current was concentrated in a very limited latitude range. While the $\Delta B(\Phi)$ pattern might be interpreted as a basic two region pattern, the magnetometer current density shows structure with current reversals even in this one second averaged data, which certainly dominates over any average current within any region. Again there is remarkable agreement in the upward current pattern between the electron and magnetometer calculated currents, and in the largest burst, even excellent agreement in magnitude. The majority of the current carried by the suprathermal electrons lies in the energy range 120 to 480 eV.

ORIGINAL PAGE IS
OF POOR QUALITY

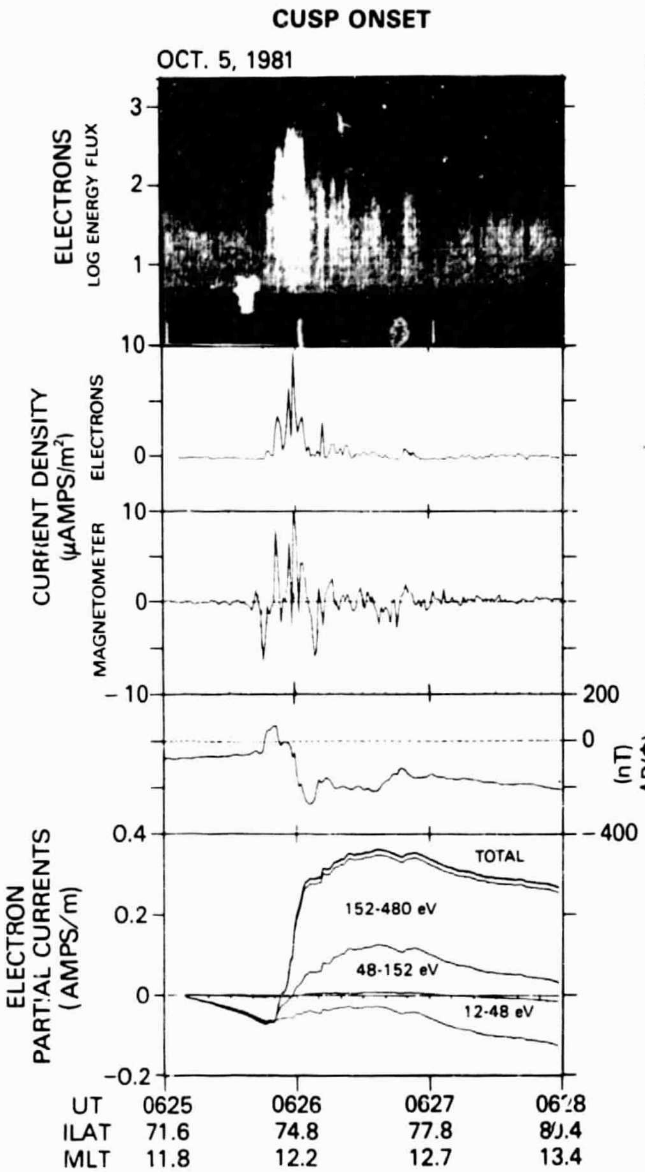

Fig. 10. Data from a cusp pass during the onset of a substorm in a format similar to Figure 2.

From a study of about 20 onset events, we have come to the following conclusions pertaining to the relationships between the precipitating particles and the field-aligned currents:

General:

1. Region 1 and Region 2 currents are clearly evident.

2. Current density fine structure within a region is larger in magnitude than the average current of the region.

3. >5 eV electrons carry the order of 50% of the upward current.

4. The suprathermal electron current carrying range extends from above photoelectron energies to a few keV.

Dusk:

1. Region 1 (upward) and Boundary Plasma Sheet (BPS) coincide.

2. Region 2 (downward) and Central Plasma Sheet (CPS) low latitude boundaries are not coincident.

3. Inverted-V electrons are dominant current carriers.

RECOVERY

During the recovery phase of a substorm, the dusk sector current patterns depend both upon the local time and the length of time into the recovery period, as well as the uniqueness of each individual substorm. The first example (Figure 11 left) at 20 to 21 MLT occurred when the field was half recovered. It shows characteristics similar to an onset pass, with well defined BPS and CPS and two prominent current regions, evident from the divergent upward and downward magnetometer current sums (bottom panel). Again the upward current region (Region 1) was exactly coincident with the BPS, with the dominant current from two structures, an Inverted-V at the polar cap boundary and a BPS/CPS boundary structure too narrow to define. Within Region 2, there were many current reversals, with the largest current density at 0634 UT in the opposite direction from the normal regional current.

For the 19 MLT pass in Figure 11 (right), when the substorm had mostly recovered, the fine structure, as seen in the magnetometer current density, dominated over the trend towards two current regions (the upward and downward magnetometer current sums do not diverge as for the Sept. 30 pass). The agreement in magnitude between the two computed current densities is very poor in this case, except for the Inverted-V at 2350 UT. The remainder of the current carrying structures both in the BPS and CPS were suprathermal bursts, not the keV electrons of the diffuse (CPS) auroral region.

Looking at the partial currents for these two passes, we see in general the currents were carried by electrons over a broad energy range. However, in both cases the accelerated electrons in the Inverted-Vs were primary contributors to the current. For the pass on Sept. 30, more characteristic of an onset pass, the upward to downward current ratio in Region 1 was about 22, but the inverse ratio in Region 2 was less than 2. In contrast, the ratios for the second example were 1.3 and 1.9 respectively, again illustrating the importance of the fine structure.

The dawn recovery example (Figure 12) was taken after the substorm had nearly recovered. It shows a patchy mantle auroral region followed by a highly structured region of suprathermal bursts. Some of these bursts extended back into the mantle region with decreasing energy and current /12/. Note the rather linear increases in the separate summations of the upward and downward currents across the auroral oval, again illustrating that the fine structure dominated over any current regions.

Looking at the integrals of the partial currents in the bottom panel of Figure 12 we see that electrons in the few hundred eV energy range were the primary current carrying electrons, but these electrons carried less than half of the upward current measured by the magnetometer. This is a typical case when suprathermal bursts are the dominant electron precipitation structure. Also note that the 1.5 to 4.8 keV mantle auroral electrons did carry a small net current.

The cusp pass in Figure 13 occurred about half way into the recovery period, and while the magnetic field east-west component indicates two general regions of current, there is again considerable structure. The ratio of Region 1 (0622 to 0623.3 UT) currents was 3.1 and Region 2 (0623.3 to 0624 UT) currents was only 1.9. Surprisingly in this case, the particle detectors measured a larger current than that derived from the magnetometer data with again energies up to about 500 eV the current carriers.

From a study of about 55 passes taken during the recovery period, we arrive at the following conclusions:

Dusk:
1. From the cusp to ~1900 MLT the fine structure currents greatly exceed the average in each current region.

2. From ~1900 MLT to the Harang discontinuity the current patterns are similar to the onset period.

Dawn:
1. Region 2 is more defined spatially and has less structure than Region 1.

2. Mantle auroral electrons (keV) carry weak but widespread current.

3. Suprathermal bursts overlap with mantle auroral region and carry Region 2 current.

General:
1. The >5 eV electrons carry the order of 50% of the upward current.

2. The suprathermal electron current carrying range extends from above photoelectron energies to ~500 eV.

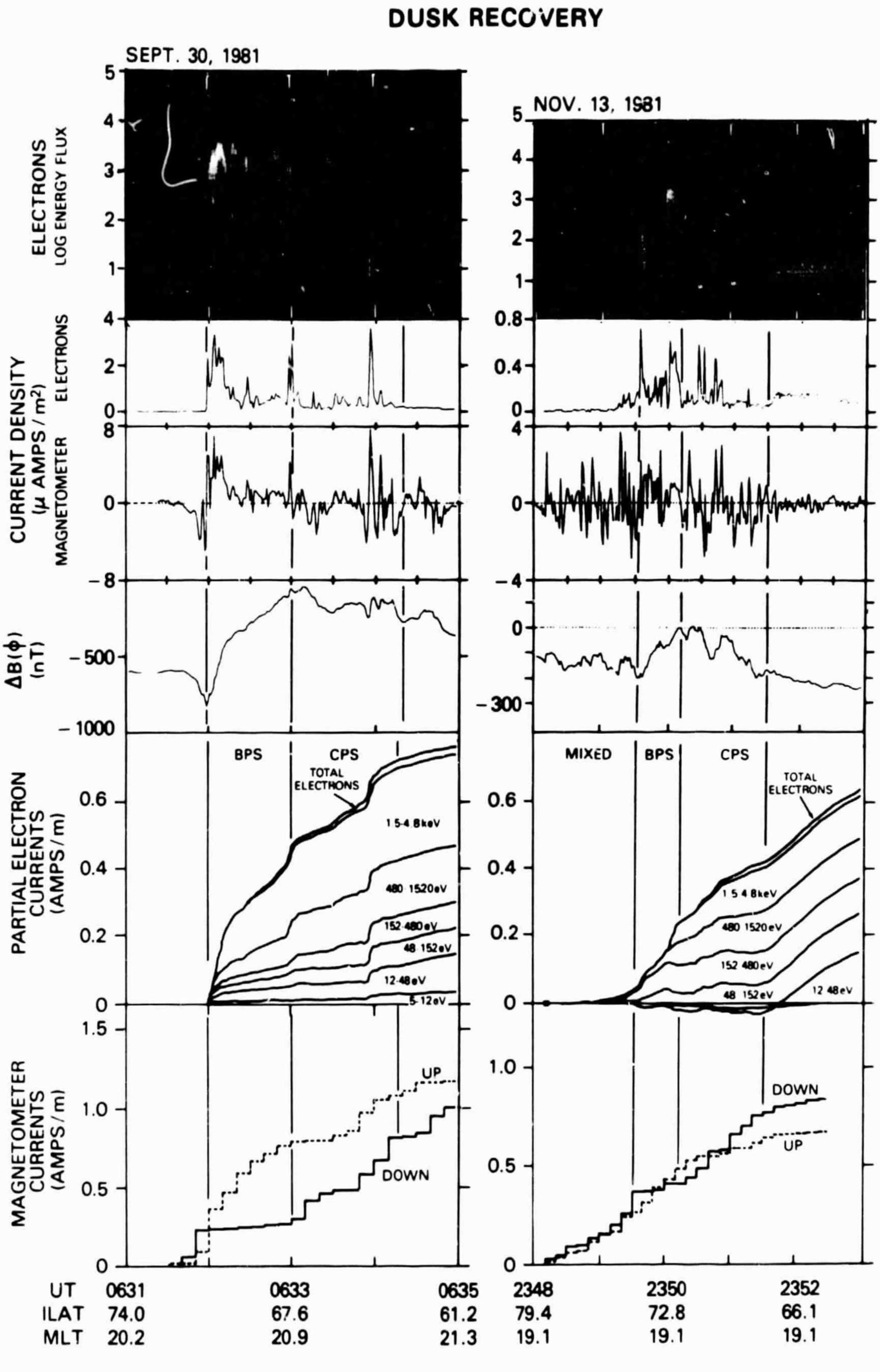

Fig. 11. Examples of data during the recovery phase from two passes through the dusk auroral oval in a format similar to Figure 2.

DAWN RECOVERY (0950 MLT)

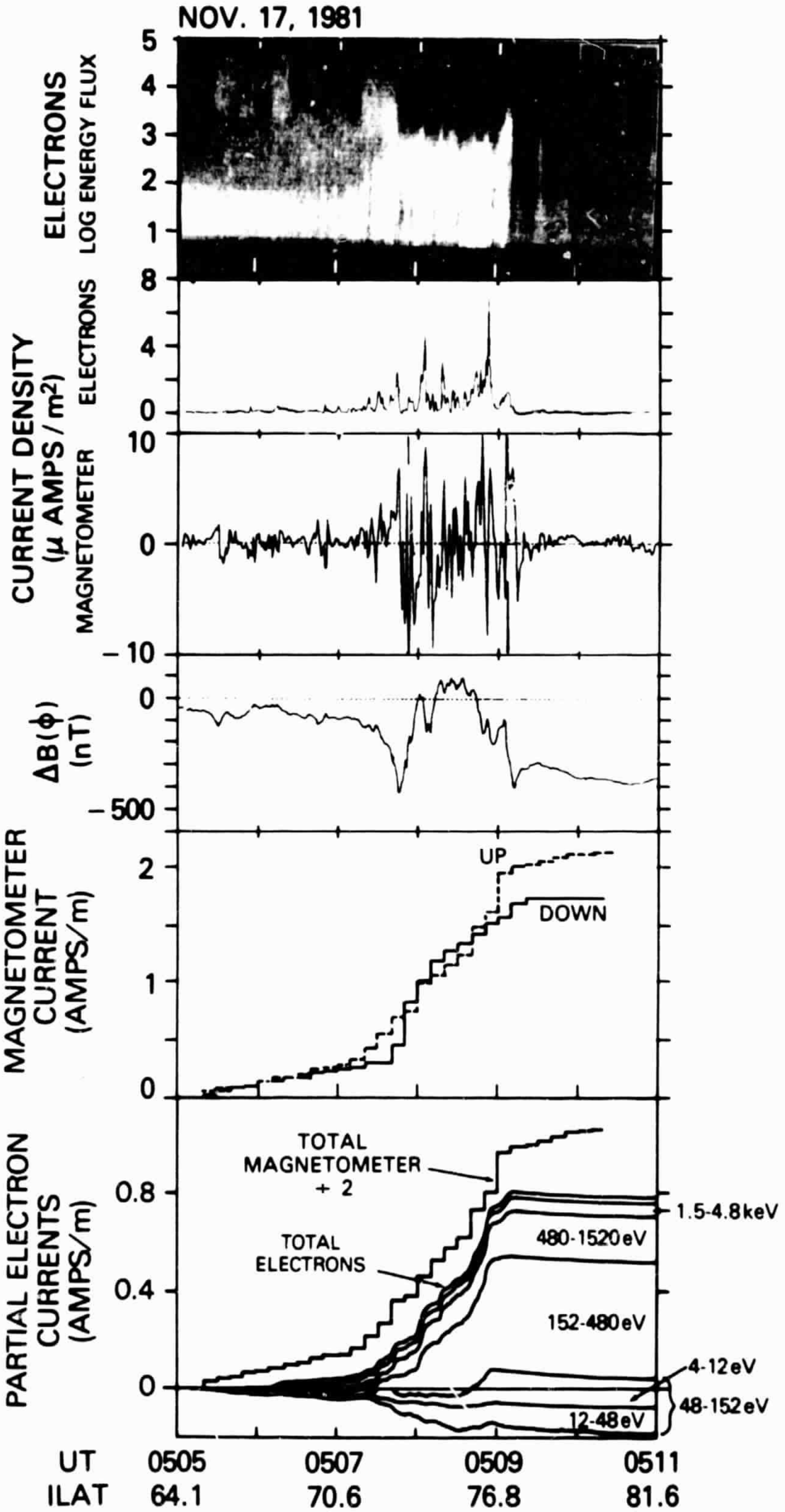

Fig. 12. Data from a dawn pass taken after a substorm had nearly recovered. Format similar to Figure 2.

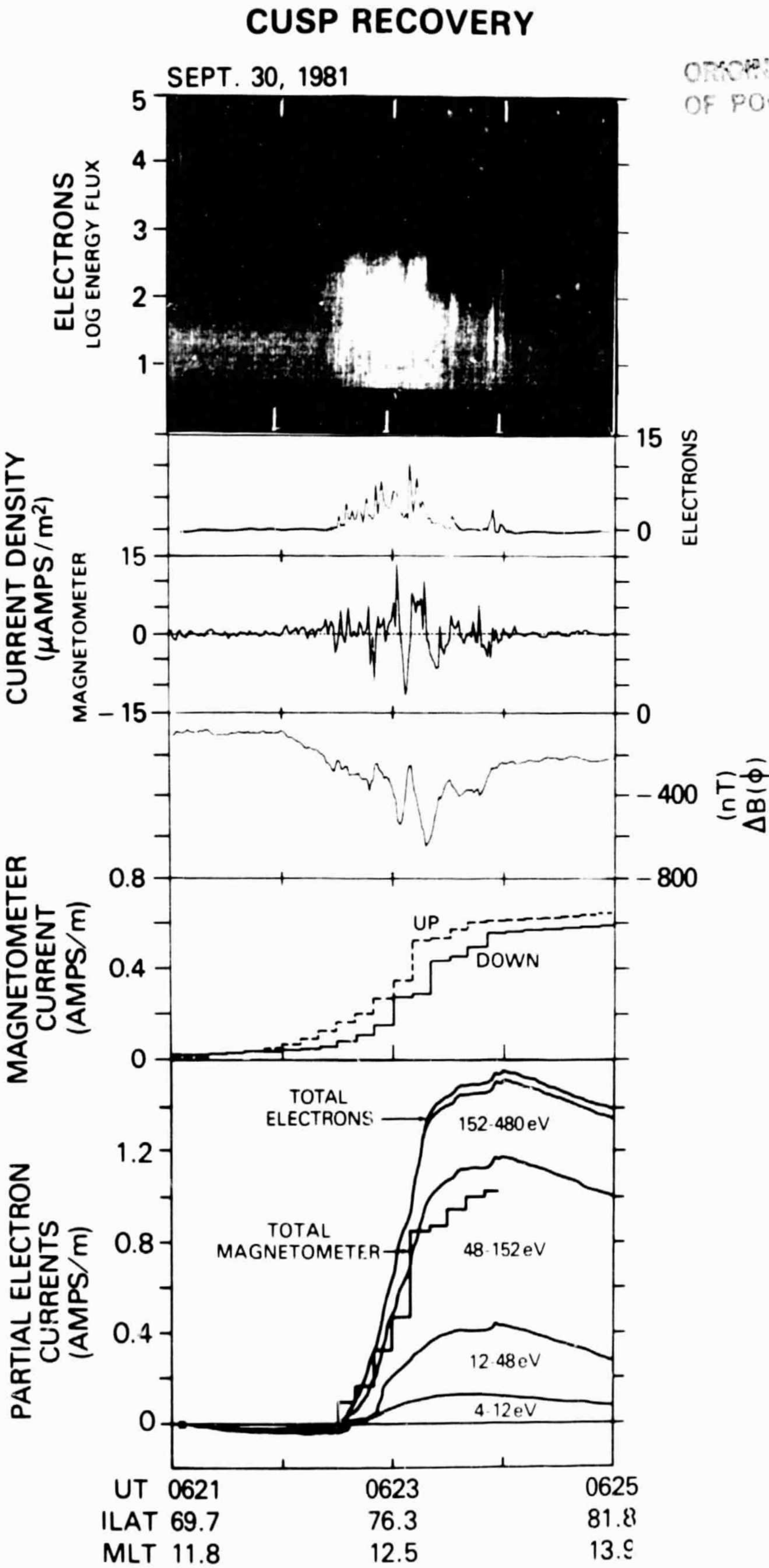

Fig. 13. Data from a pass through the cusp sector during a recovery period. Format similar to Figure 2.

DISCUSSION

In our studies to date we have not encountered any ion fluxes sufficiently intense to carry significant currents, nor upward electron beams at the altitudes of the DE-2 satellite which would carry downward currents. However, Heelis et al /14/ have reported vertical ion drifts of sufficient velocity and density to carry currents in excess of 10^{-5} Amps/m^2. At much higher altitudes using data from the DE-1 satellite there have been two reports of upward electron fluxes carrying significant currents. Burch et al /15/ found that intense upward electron beams with energies from ~20 eV to ~200 eV are a common feature of the region just equatorward of the morning-side polar cusp. Computations of the currents carried by these beams and by the precipitating cusp electrons showed agreement with the simultaneous magnetometer measurements for both upward and downward Birkeland currents. The data indicate that the cold ionospheric electrons which carry the downward Region-1 currents on the morning side are accelerated upward by potentials of a few tens of eV at altitudes of several thousand kilometers. In the nighttime auroral zone at altitudes of about 2 earth radii, Lin et al /16/ have reported that type-1 counterstreaming electrons can carry sufficient current density to account for small scale downward currents. These two observations at high altitudes seem to confirm the assumption that at low altitudes the downward electric currents are carried by thermal electrons moving up and out of the ionosphere.

On the basis of the observations made with instruments of the DE-2 spacecraft, we summarize our conclusions regarding the distribution and carriers of field-aligned currents at low altitudes:

1. During very quiet periods, field-aligned currents exist primarily as fine structure.
2. During onset, Region 1 and Region 2 become clearly evident but contain significant structure.
3. As magnetic activity subsides, current regions become less distinct, and fine structure becomes more dominant.
4. The distribution of the upward currents derived from magnetometer data and calculated from suprathermal electron data agree remarkably well in shape but not necessarily in magnitude.
5. At all local times, >5 eV electrons seldom carry most of the upward current.
6. Except for the accelerated Inverted-V electrons, the dominant upward current carriers which are measured are electrons below 500 eV and are distributed in energy.
7. Dusk upward currents (Region 1) are associated with the Boundary Plasma Sheet (BPS).
8. Suprathermal electron bursts are important current carrying structures.

ACKNOWLEDGEMENT

The authors are grateful to Dr. J. R. Thieman for considerable graphics and analysis support pertaining to the field-aligned currents derived from the low altitude plasma data.

REFERENCES

1. B.M. Shuman, R.D. Vancour, M. Smiddy, N.A. Saflekos and F.J. Rich, Field-Aligned Current, Convective Electric Field and Auroral Particle Measurements During a Major Magnetic Storm, J. Geophys. Res., 86, 5561 (1981).

2. D.M. Klumpar, J.R. Burrows and M.D. Wilson, Simultaneous Observations of Field-Aligned Currents and Particle Fluxes in the Post-Midnight Sector, Geophys. Res. Lett., 3, 395 (1976).

3. N.A. Saflekos, R.E. Sheehan and R.L. Carovillano, Global Nature of Field-Aligned Currents and Their Relation to Auroral Phenomena, Rev. Geophys. Space Phys., 20, 709 (1982).

4. D.M. Klumpar and W.J. Heikkila, Electrons in the Ionospheric Source Cone: Evidence for Runaway Electrons as Carriers of Downward Birkeland Currents, Geophys. Res. Lett., 9, 873 (1982).

5. T.A. Potemra, Current Systems in the Earth's Magnetosphere, Rev. Geophys. Space Phys., 17, 640 (1979).

6. T.A. Potemra, Editor, Magnetospheric Currents, Geophysical Monograph 28, American Geophysical Union, Washington, D.C., 1984.

7. R.A. Hoffman and E.R. Schmerling, Dynamics Explorer Program: an overview, Space Sci. Instr., 5, 345 (1981).

8. W.H. Farthing, M. Sugiura, B.G. Ledley and L.J. Cahill, Jr., Magnetic Field Observations on DE-A and -B, Space Sci. Instr., 5, 551, (1981).

9. J.D. Winningham, J.L. Burch, N. Eaker, V.A. Blevins, and R.A. Hoffman, The Low Altitude Plasma Instrument (LAPI), Space Sci. Instr., 5, 465 (1981).

10. J.D. Winningham, F. Yasuhara, S.-I. Akasofu and W.J. Heikkila, The Latitudinal Morphology of 10-eV to 10-keV Electron Fluxes During Magnetically Quiet and Disturbed Times in the 2100-0300 MLT Sector, J. Geophys. Res., 80, 3148 (1975).

11. R.A. Hoffman, Properties of Low Energy Particle Impacts in the Polar Domain in the Dusk and Dayside Hours, in: Magntosphere-Ionosphere Interactions, ed. K. Folkestad, Universitetsforlaget, Oslo, 1972, p. 117.

12. A.D. Johnstone and J.D. Winningham, Satellite Observations of Suprathermal Electron Bursts, J. Geophys. Res., 87, 2321 (1982).

13. M. Sugiura, T. Iyemori, R.A. Hoffman, N.C. Maynard, J.L. Burch and J.D. Winningham, Relationships Between Field-Aligned Currents, Electric Fields, and Particle Precipitation as Observed by Dynamics Explorer-2, in: Magnetospheric Currents, ed. T.A. Potemra, American Geophysical Union, Washington, D.C., 1984, p. 96.

14. R.A. Heelis, J.D. Winningham, M. Sugiura and N.C. Maynard, Particle Acceleration Parallel and Perpendicular to the Magnetic Field Observed by DE-2, J. Geophys. Res., 89, 3893 (June 1984).

15. J.L. Burch, P.H. Reiff and M. Sugiura, Upward Electron Beams Measured by DE-1: A Primary Source of Dayside Region-1 Birkeland Currents, Geophys. Res. Lett., 10, 753 (1983).

16. C.S. Lin, M. Sugiura, J.L. Burch, J.N. Barfield and E. Nielsen, DE-1 Observations of Type-1 Counterstreaming Electrons and Field-Aligned Currents, accepted for pub. J. Geophys. Res., (1984).